Phys. Status Solidi C **11**, No. 3–4, 887–889 (2014) / **DOI** 10.1002/pssc.201300668

physica status solidi c
www.pss-c.com
current topics in solid state physics

AlGaN/GaN HEMTs on Si by MBE with regrown contacts and f_T = 153 GHz

Satyaki Ganguly[*,1], Bo Song[1], Wan Sik Hwang[2], Zongyang Hu[1], Mingda Zhu[1], Jai Verma[1], Huili (Grace) Xing[1], and Debdeep Jena[1]

[1] Department of Electrical Engineering, University of Notre Dame, Notre Dame, IN 46556, USA
[2] Department of Materials Engineering, Korea Aerospace University, 76 Hanggongdaehang-ro, Deogyang-gu Goyang-City, Gyunggido 412-791, Korea

Received 14 October 2013, accepted 24 January 2014
Published online 24 March 2014

Keywords GaN, HEMTs, MBE, regrown

* Corresponding author: e-mail sganguly@nd.edu, Phone: +1 574 631 1290, Fax: +1 574 631 4393

AlGaN/GaN high-electron-mobility transistors (HEMT) have been grown by radio frequency molecular beam epitaxy (RF-MBE) on 3" Si substrates. A record low contact resistance R_c ~ 0.11 Ω.mm has been achieved for GaN HEMTs on Si by using non alloyed ohmic contacts regrown by MBE. Owing to the low contact resistance a 75-nm gate length unpassivated HEMT shows intrinsic current gain cut-off frequency f_T=153 GHz, a high saturation drain current density> 1.3 A/mm and a low R_{ON} of 1 Ω.mm, among the best reported for HEMTs on Si. With further scaling GaN HEMTs on Si can compete in the high-performance RF arena with similar devices on SiC, while exploiting the many advantages of integration with Si.

1 Introduction Large-area and low-cost Si wafers have proven attractive as substrates for GaN power electronics [1]. Due to their desirable power handling capability low-Al-composition (<40%) AlGaN/GaN-based HEMTs are finding many high-power and high-frequency applications [2]. The large lattice and thermal mismatch makes the epitaxy of AlGaN/GaN HEMTs on Si substrates challenging. Nevertheless, high performance devices were reported recently where f_T and f_{max} exceeded 140 GHz with a DC output current density > 1.0 A/mm [3, 4]. To improve the device performance further with ultra-scaled geometries, it is highly desirable to minimize the contact resistance since it generally dominates the total parasitic resistance. Molecular Beam Epitaxy (MBE) regrown contacts [5] have been employed recently in GaN HEMTs, resulting in a performance boost in metal- and N-polar HEMTs on SiC [6, 7]. For GaN HEMTs on Si a contact resistance R_c ~ 0.27 Ω mm by MOCVD was recently reported [8], which is higher than those achieved by MBE, presumably due to the choice of different growth regime.

In this work we demonstrate the lowest R_c~0.11 Ω mm for GaN HEMTs on Si reported yet by using the MBE regrowth technique. The scaled HEMT with L_g~75 nm fabricated from AlGaN/GaN HEMTs grown on 3" high resistivity (HR)-Si wafer using RF-MBE results in an R_{ON} ~ 1 Ω mm and I_d > 1.3 A/mm, a record performance for AlGaN family of HEMTs on Si. Owing to the record low contact resistance, AlGaN/GaN HEMTs with barrier thickness as high as ~22 nm, is able to deliver a current gain cut-off frequency f_T~ 153 GHz. Such speeds for GaN HEMTs on Si were achieved with much thinner barriers earlier [3, 9]. The thicker barrier used here enables a higher current on/off ratio because of low gate leakage currents. The low on-resistance enabled by MBE regrown contacts is expected to reduce unwanted power losses for both high power and high-speed devices for GaN HEMTs on Si.

2 Device structure and fabrication The heterostructures were grown on HR (>10^4 Ω cm) 3" 525 µm Si (111) substrates by MBE in a Veeco Gen 930 system. The MBE growth of AlGaN HEMTs on Si initiates with an AlN nucleation layer to prevent the 'melt back etching' problem [10] and to reduce the thermally induced tensile stress to avoid cracking. The growth conditions of the metal-polar 2 nm GaN cap/20 nm $Al_{0.32}Ga_{0.68}N$/ 1.5 µm GaN/100 nm AlN/Si (111) samples were tuned to ensure smooth 2D layers with a ~0.6 nm rms roughness measured over 2 µm × 2 µm scans. A schematic epilayer

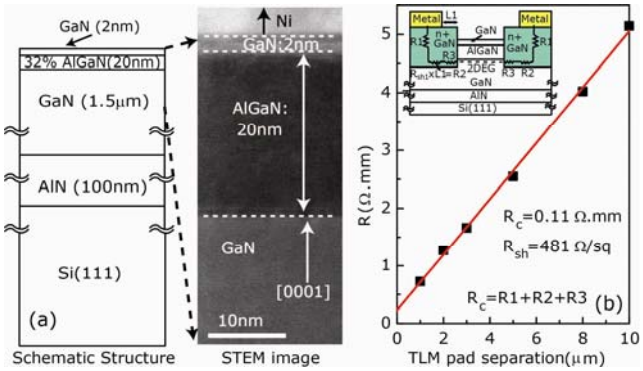

Figure 1 (a) Schematic of the layer structure and the corresponding STEM image showing the barrier layer thickness along with the GaN buffer layer; (b) TLM (regrown contact on AlGaN HEMTs channel) fitting for the HEMTs structure measured at RT. Schematic of the MBE regrown contact TLM pattern on the heterostructure is shown in the inset.

structure and a corresponding scanning transmission electron microscopy (STEM) image of the as grown HEMT active regions are shown in Fig. 1(a). Hall-effect measurements at RT showed a μ~1006 cm^2/Vs 2DEG mobility of density n_s~1.44 × 10^{13} cm^{-2}. The details of epitaxial growth and material characterization will be presented elsewhere.

The device fabrication initiated with patterning of a SiO_2 mask for the n+ GaN ohmic regrowth by MBE. Using BCl_3 (30 sccm) gas at a 40 V DC voltage the S/D regions were etched ~50 nm removing the AlGaN barrier, and a 100 nm heavily doped n+ GaN was regrown by MBE in a metal rich growth condition. A substrate thermocouple temperature of 660 °C was used for the regrowth. The Si doping density in the regrown contact region was ~10^{20} cm^{-3} calibrated by transport and SIMs data. The S/D regrown regions were separated by ~1 μm. Following regrowth the poly-GaN deposited on top of SiO_2 was lifted off by BHF. Non-alloyed Ti/Au (20/100 nm) stack was deposited, followed by mesa isolation using Cl_2 based plasma etching. Although there are lower work function metals available, Ti is chosen here since it is known to reduce the native oxide on the GaN surface, thus leaving no insulating oxide at the interface and promoting a more intimate contact. Finally, 75-nm Ni/Au (20/70 nm) rectangular gates were defined by electron-beam lithography and deposition without recess or any additional dielectrics. The resulting device reported here thus has W = 2x50 μm, L_g = 75 nm, L_{sg} = 175 nm, L_{gd} = 750 nm and L_{sd} = 1 μm.

3 Results and discussion Transmission line method (TLM) measurements were used to investigate the regrown n+GaN electrical characteristics on the processed samples. The TLM gaps between regrown n+ GaN wells were measured by scanning electron microscopy (SEM). Fig. 1(b) shows the results. The schematic of the structure and the contacts are shown in the inset of Fig. 1(b). From the TLM patterns with the HEMT channel and regrown contacts, R_c ~ 0.11 Ω mm and R_{sh} ~ 481 Ω/sq were extracted. From TLM patterns on the regrown n+ GaN regions, R_{c1} ~ 0.05 Ω mm and R_{sh1} ~ 42 Ω/sq were obtained. For a $L1$ ~ 400 nm distance between the regrown region and the metal edge the resistance between the regrown n+ GaN and the 2DEG channel is thus extracted to be ~0.05 Ω mm, similar to our prior reports for InAlN HEMTs on SiC [11]. This R_c value is the lowest reported for GaN HEMTs on Si- which is ~2X lower than the previous best report [12] of 0.18 Ω mm. Figure 2(a) shows the DC common source characteristics of the device. A saturation drain current density I_d > 1.3 A/mm is obtained for V_{gs} = 1 V and V_{ds} = 6 V. The output conductance observed is possibly due to the less-than ideal L_g/t_b < 4 ratio.

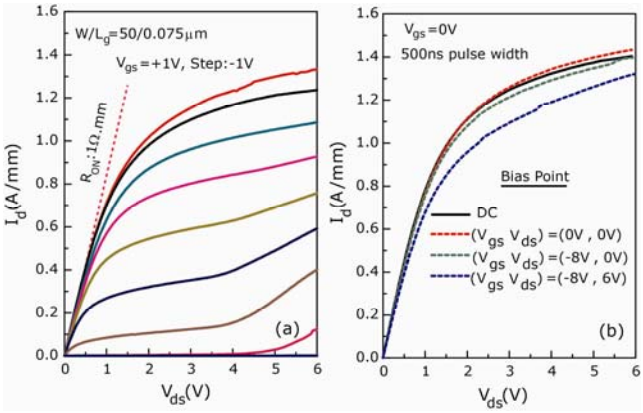

Figure 2 (a) DC common source family of I-V's showing R_{on} = 1 Ω·mm. (b) Pulsed I-V measurement at V_{gs}=0, with a 500-ns pulse width and a 0.5-ms period of the same device shown in (a).

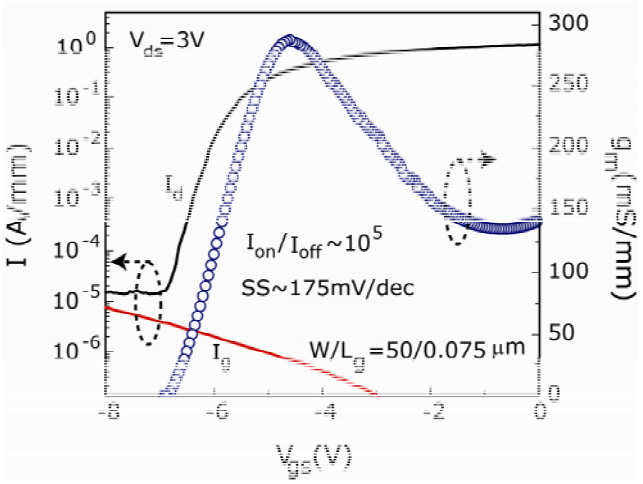

Figure 3 Transfer characteristics of the AlGaN/GaN HEMTs are plotted indicating $g_{m,ext}$ = 290 mS/mm.

The device R_{ON} is extracted to be 1 Ω mm, the best reported for the HEMTs on Si, owing to the very low MBE-regrown contact resistance. This R_{ON} value is slightly higher than the sum of the source, drain and channel resistances (0.7 Ω mm) calculated based on the four-probe TLM measurement data. Pulsed I–V measurements were performed in air using a 500-ns pulse width and a 0.5-ms period, as shown in Fig. 2(b). Even without conventional SiN passivation, little dispersion was observed in the pulsed I-V measurement, thanks to the non-alloyed regrown ohmic contacts that allow the free surface of the GaN HEMTs to be similar to the as-grown surface with minimal exposure to high temperature process.

The DC transfer characteristics of the device are shown in Fig. 3. A peak extrinsic transconductance of $g_{m,ext}$ = 290 mS/mm was measured at V_{ds} = 3 V. In spite of short channel effects, an I_{ON}/I_{OFF} ~ 10^5 is obtained at V_{ds} = 3 V. For submicron gate length devices the tree terminal breakdown voltage (not shown here) was measured to be ~22V, where I_d=1 mA/mm is set as the breakdown limit.

On-wafer RF measurements were taken from 250 MHz to 30 GHz at the peak f_T bias condition. The network analyzer was calibrated using an off-wafer impedance standard. The on-wafer open and short structures were used to de-embed the pad parasitics from the measured S-parameters. Figure 4 shows the current gain $|h_{21}|^2$ and power gain U of the HEMT as a function of the frequency at the peak f_T bias condition, V_{ds} = 4.5 V, and V_{gs} = -5.25 V. The extrapolation of $|h_{21}|^2$ and U with a -20 dB/dec roll off yields f_T = 153 GHz and f_{max} = 22 GHz after de-embedding. The high gate resistance of the rectangular gate causes a lower f_{max} than what is attractive for high power millimeter-wave applications. This issue will be addressed using T-shape gates in the future. The top view SEM image indicating the device dimensions is shown in the inset of Fig.4. The f_T reported here is among the best for GaN HEMTs on Si [3] but with higher on/off ratio, lower contact resistance, and lower on-resistance as a consequence of the first integration of MBE-regrown contacts with GaN HEMTs on Si.

4 Conclusions In conclusion, in this work we have demonstrated 75-nm gate length AlGaN/GaN HEMTs grown on (111) high-resistivity Si substrates by RF MBE with peak current gain cutoff frequency f_T = 153 GHz, saturation drain current density in excess of 1.3 A/mm and R_{ON} as low as 1 Ω.mm. By employing MBE regrown contacts, record low R_c ~ 0.11 Ω.mm has been obtained for GaN HEMTs on Si. The attractive DC and RF performances are attributed to the low-resistance ohmic contacts. The low on-resistance is attractive for reducing losses in high power and high frequency microwave applications, and mitigating the problem of the low- thermal conductivity of Si compared to SiC. With thinner barriers and further device scaling, integration of MBE regrown contacts with GaN on Si HEMT platform thus offers pathways to boost the performance and efficiency of high-power and high-speed devices while harvesting the many advantages of being on a Si platform.

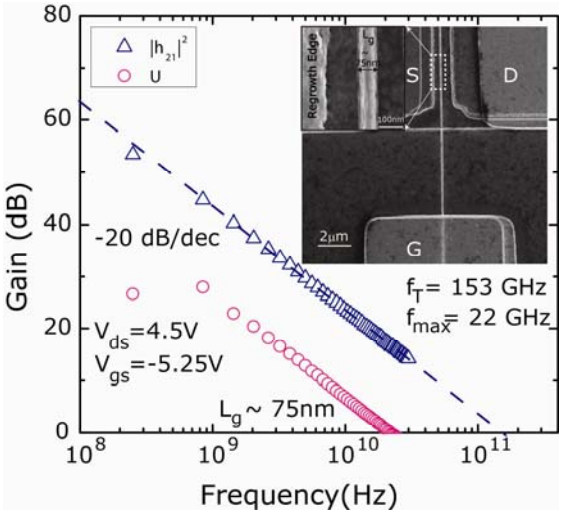

Figure 4 Small signal RF characteristics of the AlGaN/GaN HEMTs showing f_T = 153 GHz and f_{max} = 22 GHz. The top view SEM image indicating the device dimensions is shown in the inset.

References

[1] M. Higashiwaki, T. Mimura, and T. Matsui, Proc. SPIE **6894,** 68941L-1 (2008).
[2] U. K. Mishra, L. Shen, T. E. Kazior, and Y.-F. Wu, Proc. IEEE **96,** 287 (2008).
[3] D. Marti, S. Tirelli, A. R. Alt, J. Roberts, and C. R. Bolognesi, IEEE Electron Device Lett. **33,** 1372 (2012).
[4] F. Medjdoub, B. Gimbert, D. Ducatteau, and N. Rolland, Appl. Phys. Express **6,** 044001 (2013).
[5] J. Guo, Y. Cao, C. Lian, T. Zimmermann, G. Li, J. Verma, X. Gao, S. Guo, P. Saunier, D. Jena, and H. Xing, Phys. Status Solidi A **208,** 1617 (2011).
[6] S. Dasgupta, Nidhi, D. F. Brown, F. Wu, S. Keller, J. S. Speck, and U. K. Mishra, Appl. Phys. Lett. **96,** 143504 (2010).
[7] K. Shinohara, A. Corrion, D. Regan, I. Milosavljevic, D. Brown, S. Burnham, P. J. Willadsen, C. Butler, A. Schmitz, D. Wheeler, A. Fung, and M. Micovic, IEDM Tech. Dig., p. 30.1. (2010),
[8] T. Huang, X. Zhu, and K. M. Lau, IEEE Electron Device Lett. **33,** 1123 (2012).
[9] H. Sun, A. R. Alt, H. Benedickter, C. R. Bolognesi, E. Feltin, J. F. Carlin, M. Gonschorek, and N. Grandjean, Appl. Phys. Express **3,** 094101 (2010).
[10] A. Krost and A. Dadgar, Phys. Status Solidi A **208,** 361 (2002).
[11] J. Guo, G. Li, F. Faria, Y. Cao, R. Wang, J. Verma, X. Gao, S. Guo, E. Beam, A. Ketterson, M. Schuette, P. Saunier, M. Wistey, D. Jena, and H. Xing, IEEE Electron Device Lett. **33,** 525 (2012).
[12] S. Arulkumaran, G. I. Ng, S. Vicknesh, H. Wang, K. S. Ang, C. M. Kumar, K. L. Teo, and K. Rajan, Appl. Phys. Express **6,** 016501 (2012).